STEPHY Publishers

Trends in Petroleum Engineering

Research Article

ISSN: 2771-2494

Lateral Rock Characteristic Evidence of Hydrocarbon Restoration from Post-Stack Impedance Inversion: A Case Study of ZED-field Offshore Niger Delta

John J Osazee,[1] Stanley U Eze,[2]* Omafume M Orji,[3] Onyekwere Kelechi Raymond,[3] Saleh A Saleh[3]

[1]Department of Physics, University of Benin, Nigeria

[2]Department of Earth Sciences, Federal University of Petroleum Resources, Nigeria

[3]Department of Petroleum Engineering and Geosciences, Petroleum Training Institute, Nigeria

Abstract

Lateral predictions of rock properties that are descriptive of a reservoir have been studied using a model-established seismic inversion approach that was used to convert input seismic data into an acoustic impedance structure to optimize hydrocarbon restoration in the field. This was actualized by integrating wireline logs and 3D post stack seismic data procured from ZED-Field offshore Niger Delta. The inversion system employed in this study comprises of forward modelling of reflection coefficients starting with a low-frequency impedance model induced from well logs and convolution of the reflection coefficients with the source wavelet extracted from the seismic input. P-impedance analysis at reservoir C5000 delineated from the control well gave a near perfect correlation of 0.998109 (≈ 99.8 %) between the original P-impedance log, initial P-impedance model log and inverted P-impedance log with an estimated error of 0.0616932 which is about (6.16%). Seismic inversion analysis realized an acoustic impedance structure with P-impedance values ranging from 3801 to 11073.0m/s*g/cc and having an overall increase with depth tendency. Specifically, a low-impedance structure was observed at the reservoir window that can be profiled laterally elsewhere from the existing wells. Impedance slices extracted from the impedance volume at the top and base of reservoir C5000 clearly showed low impedance values away from the existing wells which are evidence of new hydrocarbon prospects (hydrocarbon-charged sands) in the field that can be explored for improved hydrocarbon recovery and field development. Therefore, the realized attribute could supply litho-fluids knowledge inside the current reservoirs, and likewise aid in defining probable hydrocarbon regions of low impedance that can be tested with the input seismic to boost the interpretation of reservoir attributes with feasible integration to seismic stratigraphy for improved reservoir prediction away from the extant wells. This information can be invaluable in delineating more prospective reservoir zones in the field, and thereby enhancing optimum field development which aids in reservoir management decisions.

Keywords: Acoustic impedance, Model-based seismic inversion, Hamson Russell Software (HRS), Lateral property prediction, Hydrocarbon restoration

Introduction

One of the best methods for finding hydrocarbons is still the seismic reflection method. Reflections result from differences in the physical characteristics of rocks, such as density and compressional wave velocity, which can be evaluated in terms of lithology, porosity, and porefill. These changes in elastic properties across the geologic interface cause reflections.[1,2] Determining the structural and stratigraphic occurrence of hydrocarbon accumulations at and away from well control is the ultimate objective of the seismic approach. In order to realize relevant eventualities for hydrocarbon prediction away from existing wells and to improve field development, efforts are made in quantitative seismic interpretation to retrieve layer-based rock properties that are descriptive of a reservoir from the interface-based input seismic data using the inversion procedure.[3,4]

Quick Response Code:

***Corresponding author:** Stanley U Eze, Department of Earth Sciences, Federal University of Petroleum Resources, Effurun, Nigeria

Received: 26 April, 2024 **Published:** 08 May, 2024

Citation: John J Osazee, Stanley U Eze, Omafume M Orji, Onyekwere Kelechi Raymond, Saleh A Saleh. Lateral Rock Characteristic Evidence of Hydrocarbon Restoration from Post-Stack Impedance Inversion: A Case Study of ZED-field Offshore Niger Delta: Research Article. *Trends Petro Eng.* 2024;4(2):1–12. DOI: 10.53902/TPE.2024.04.000537

After relevant fundamental processing converts seismic traces into a pseudo reflection-coefficient time series, the seismic data (a time series) is inverted to create an acoustic impedance log. These pseudo logs are roughly parallel to the logs that are taped in the reference wells that are drilled at the field's seismic trace site.

In addition to predicting rock attributes for optimal hydrocarbon recovery, they yield important information regarding the nature of the rock and diversities in lithology of the individual geologic beds.[1]

These data are relevant for the quantitative assessment of arbitrary reservoir prospects, such as porosity, fluid content, and other petrophysical criteria to be explained in a lateral view over a given field. Careful initial processing, including wave-molding, wave-equation migration, fitting decaonvolution, true-amplitude reformation, and amplitude escalation, is required to recover the best quality pseudologs. In order to convert velocity to acoustic impedance, the low-frequency component which is absent from seismic records is added to the acoustic impedance pseudologs using reflection-moveout velocity data and a velocity-density exchange. To verify the effectiveness of the pseudologs, acoustic impedance records are arranged in wavering amplitude or color, and pseudologs are positioned in relation to acoustic logs deduced from well logs. In order to produce a thorough stratigraphic/reservoir imaging for improved hydrocarbon restoration, the process aims to extract the underlying geology from the input seismic data.[4-9]

These impedance recordings can be used to precisely examine the presence of hydrocarbons for the development of exploratory fields, and they are useful for exposing lateral lithologic modifications.

In order to optimize hydrocarbon recovery, this research focuses on acoustic impedance inversion and the interpretation of data for lateral rock characteristic prediction at the well control and distant from the control well. The research area is ZED-field situated offshore Niger Delta Figure 1a, 1b.

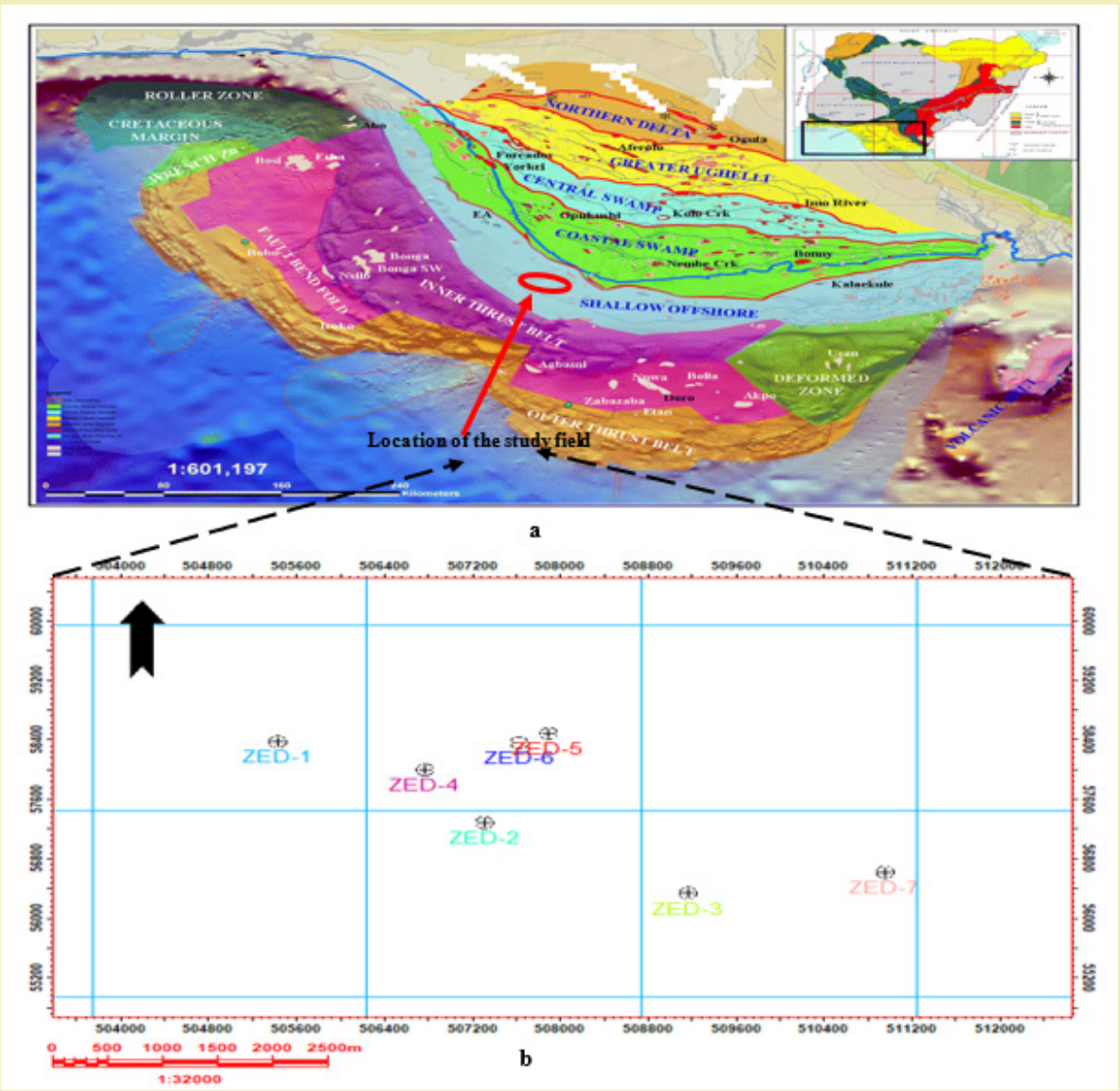

Figure 1: a: Map of the study area (ZED-Field) showing location of the study area on Niger Delta map. b: Base map of ZED-Field with seismic grid lines and well positions

Geological setting

The study area "ZED-Field" is stationed within the offshore depobelt of the Niger Delta Figure 1a. The province is a bountiful hydrocarbon region developed amid three depositional series from intervening Cretaceous to Recent. The geology, stratigraphy, and structural system of this region have been examined by the following researchers Short and Stauble,[10] Asseez,[11] and Ideozu[12] among others. The stratigraphic beds of the Niger Delta Basin incorporate the Benin, Agbada and Akata formations Figure 2. Emblematic sections of these formations are briefed in reports such as Short and Stauble,[10] and Doust and Omatsola.[13] The Akata formation is mainly composed of sea-level shale and sand layers, and its subsoil is composed of dark gray sand and shale. The thickness of this stratum is assessed to be over 7,000m.[13] The Upper Agbada formation is a series of sandstone and shale deposits.[14] It consists basically of sand within the upper part and a little amount of shale, and it contains shale within the lower portion. Over 3,700m thick, Benin's upper layers are covered in numerous places with lean layers of laterite of shifting thickness, but are more uncovered adjacent to the shoreline. It has been distinguished as recent water-bearing sand.[10,15] and all aquifers within the delta region are found inside this lithostratigraphic unit Figure 2.

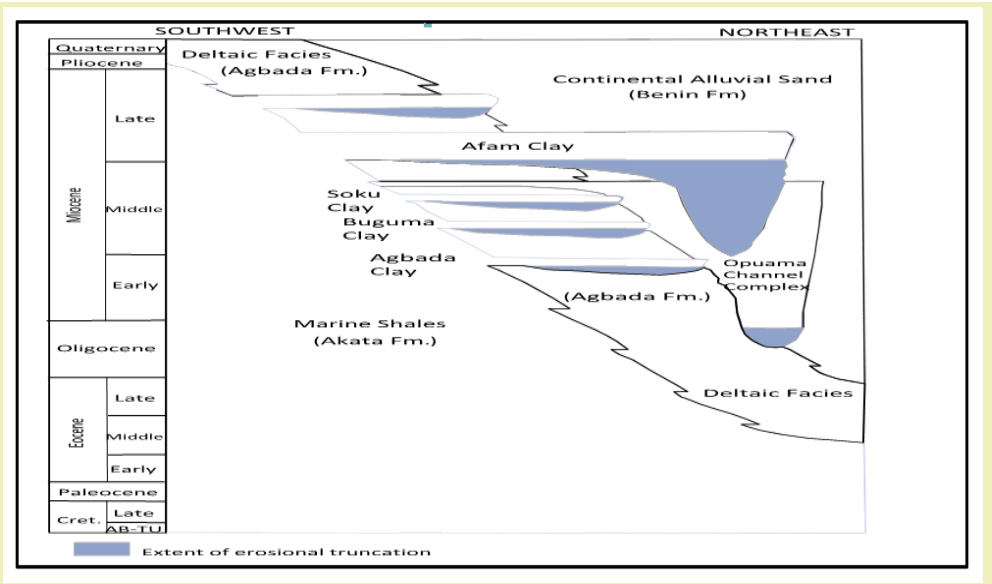

Figure 2: The three stratigraphic units of the Niger Delta (modified from Doust and Omatsola[13])

Methodology

In this study, a series of well log data from seven (7) wells that enclose Gamma-ray (GR), caliper, density, Neutron, resistivity (LLD) and compressional sonic logs and post stack seismic volume transient through the well section were utilized. The field consist of seven (7) wells named as ZED-1 to ZED-7 on the base map Figure 1b, with ZED-1 (well-01) delegated as the control well.

The model-based post stack seismic inversion technique was carried out in this study using the post stack seismic data and their associated wavelets as input.

Model-based acoustic impedance inversion

The generalized linear inversion (GLI) described by Cooke and Schneider,[16] as referenced by,[4,6,7] served as the basis for the model-based acoustic impedance inversion procedure employed in this study.

The generalized linear inversion makes use of the Taylor series expansion:

$$S(M) = S(Mi) + \frac{\partial S(Mi)}{\partial M}\Delta M + \cdots \quad (1)$$

where; Mi = initial model, M = real model, ΔM= change in model parameters, S(M) = observed seismic trace

S(Mi) = synthetic seismic from initial model

The advantage of the model-based inversion method is its capacity to minimize the difference (ΔS) between the synthetic seismic S(Mi) derived from the original model and the observed seismic trace S(M).[5] Low frequency data from nearby wells is incorporated into the original model.[5-7] Repetitive model change lowered the objective function and yields a suitable solution if the initial guess model falls inside the objective function's global consistency region.[6,7]

The objective function that was reduced is given as:

$$\mathbf{e} = (\mathbf{T} - \mathbf{wDL}) \quad (2)$$

where: **e** is the residual difference (in vector notation) between the seismic trace **T** and the trace resulting from the model data **wDL**, where **w** is the convolutional wavelet matrix for an *n* sample wavelet and L is a vector consisting of the logarithm of impedance for ***m*** model samples and given as

$$L(i) = \log Z(i) \quad (3)$$

where Z(i) is the impedance model and **D** is an *m*-1 by *m* derivative matrix where m is the amount of layers to be solved for and *m*-1 is the number of reflection coefficients.[6,7]

The addition of the square of the errors is given by:

$$e^Te=(T\text{-}wDL)^T(T\text{-}wDL) \quad (4)$$

Using the linear inverse theory,[7,17] reducing $\mathbf{e^Te}$ resulted to the "normal equation" (with a stabilization factor, a) inserted we have:

$$((D^Tw^TWD)+aI)L=D^TW^TT \quad (5)$$

However, a solution estimate was initiated by repeatedly refining an estimate of the proper model until $\mathbf{e^Te}$ is reduced, as opposed to solving Equation (5) directly for **L.**[7] Equation (5) was used to seed an initial guess model for **L**, which takes into account the low frequency trend from the accessible wells.[7,18] The low-frequency impedance information missing from the seismic data was derived from well logs, and the model was based only on the calculated impedance at log resolution from a control well, which was then predicted all through the survey domain.[6,18]

The inversion was inhibited to allow a weighting factor between reducing the sparsity of the solution and reducing the disparity of the residual traces in order to further modify the model algorithm to reflect the behavior of real rocks in the subsurface.

Reservoir delineation, Checkshot correction and well-to-seismic correlation

Reservoir C5000 was defined as the reservoir window of interest from Well ZED-1 Figure 3. Well ZED-1 (the reference well) defined the top and base of reservoir C5000.

Checkshot adjustment of the p-wave sonic log to match the two-way-time of the seismic data was the next step in the inversion process. In track 3 of Figure 4, the rectified p-wave sonic output is displayed. Track 1 Figure 4 displays the input and corrected two-way-time as black and red curves, whereas track 2 Figure 4 displays the drift curve. Using the entire stacked seismic as input, a zero-phase ricker wavelet with a length of 100ms and a frequency of 70 Hz was produced Figure 5. Next, in order to obtain a correction for the p-wave sonic velocity at the well location, the well data (ZED-1) was linked to the seismic data. The ZED-1 well (control well) was positioned above the post stack seismic volume after the post stack seismic volume (in SEG-Y format) was loaded via the HRS STRATA sub-program. To create the synthetic seismogram Figure 6, the generated wavelet was convolved with density and sonic logs from the ZED-1 well. The synthetic seismogram was linked with the composite trace (average seismic traces surrounding the well location) in an attempt to enhance the fit between the synthetic and composite trace at the well location. Using the HRS interface on the eLOG program, the correlation was carried out across the traces by selecting the stretch option. At a temporal shift of 0.00ms down, the greatest coefficient of correlation of 0.980 (≈98%) was found Figure 6.

A new P-wave sonic log was simulated after the correlation procedure. Five (5) horizons were mapped with interpolated peaks Figure 7 driven by zones of obvious seismic amplitudes on the seismogram Figure 6. The mapped horizons and control well were used as inputs to supply the geological framework drift for the inversion process. The higher the number of available wells and horizons, the better the initial model input.

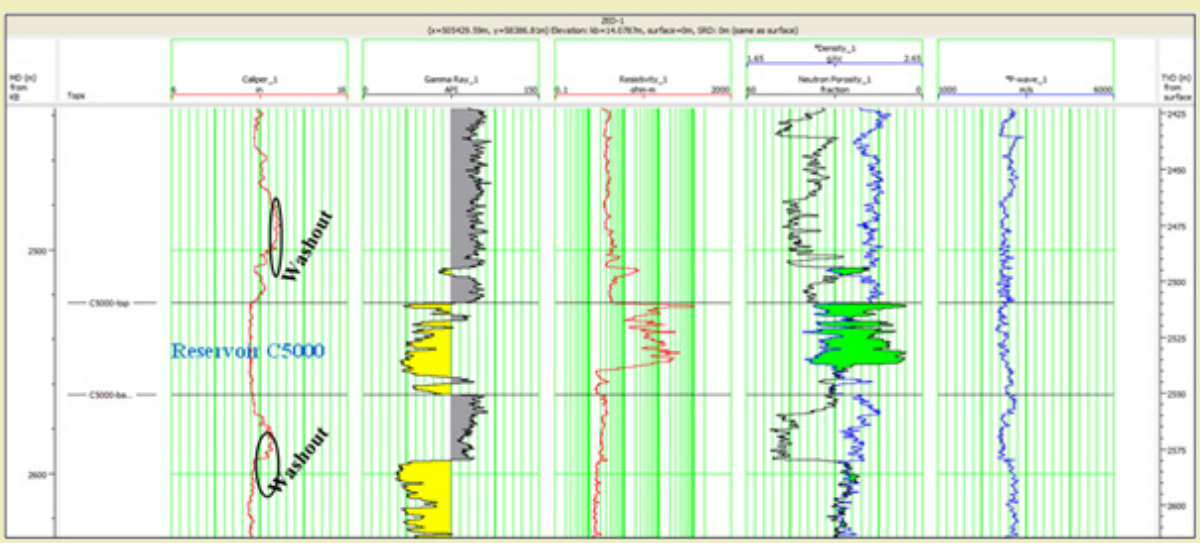

Figure 3: Log display section of reservoir C5000 across ZED-1 well showing the top and base of the reservoir window in HR software interface

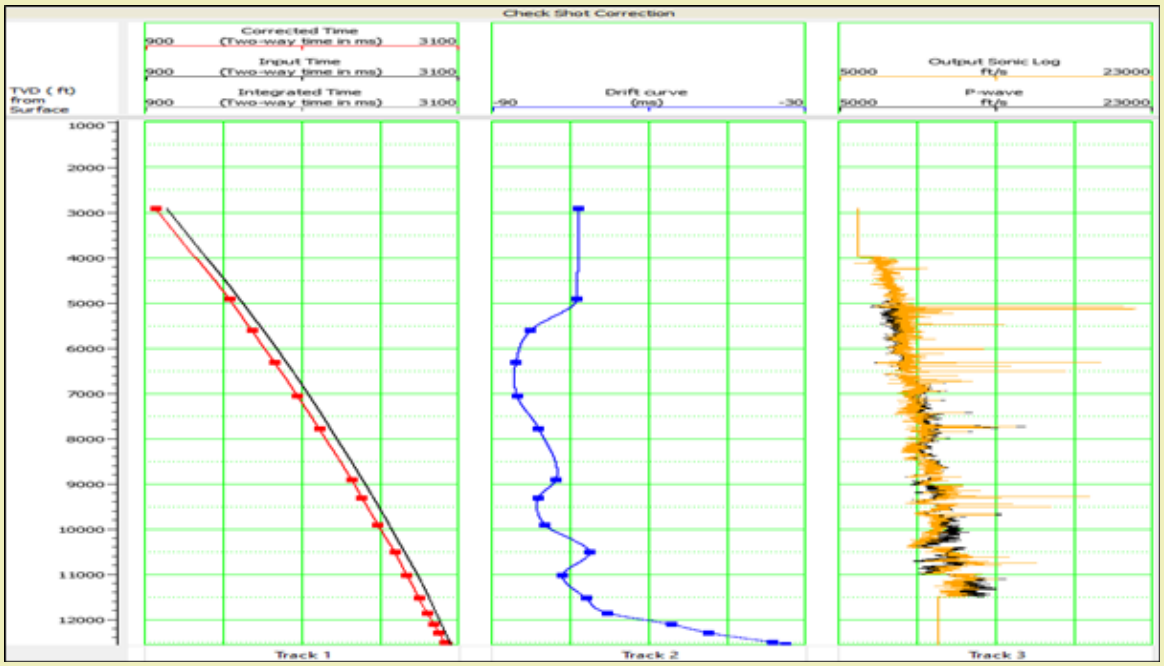

Figure 4: Check shot correction of P-waves showing the Input and corrected time (Track 1), Drift curve time (Track 2) and corrected output sonic log (Track 3)

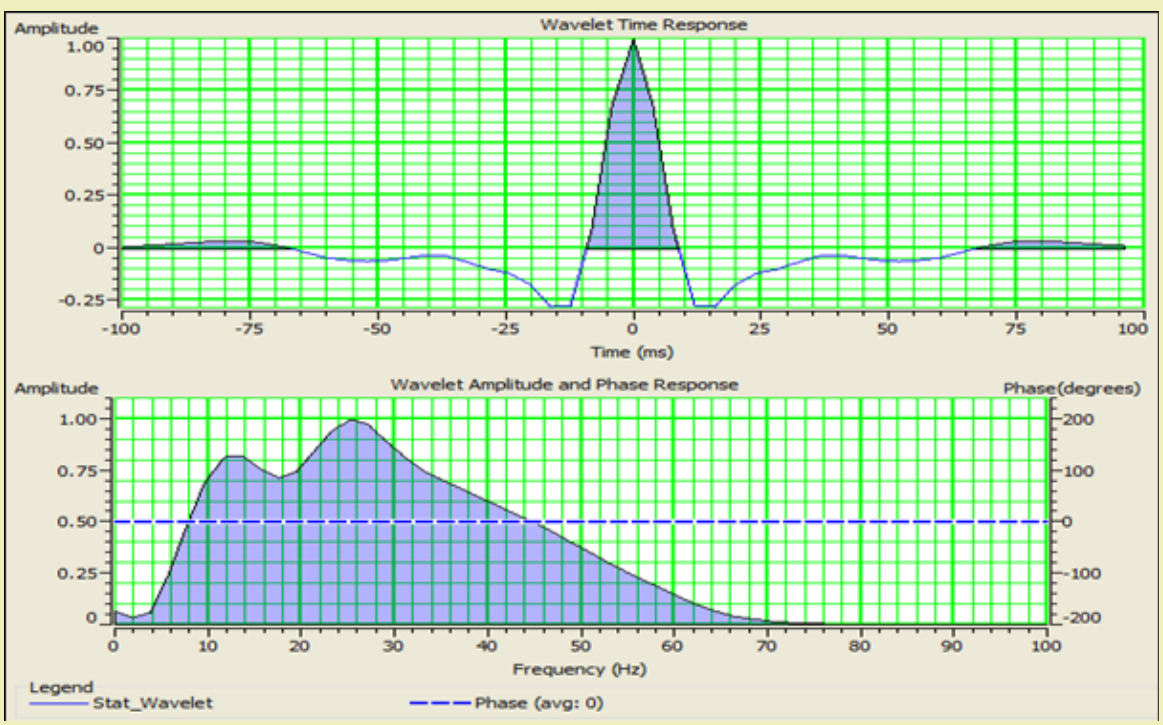

Figure 5: Extracted Seismic Wavelet in time domain and frequency domains with zero phase. The amplitude spectrum shows the approximate value of the dominant frequency (about 28Hz)

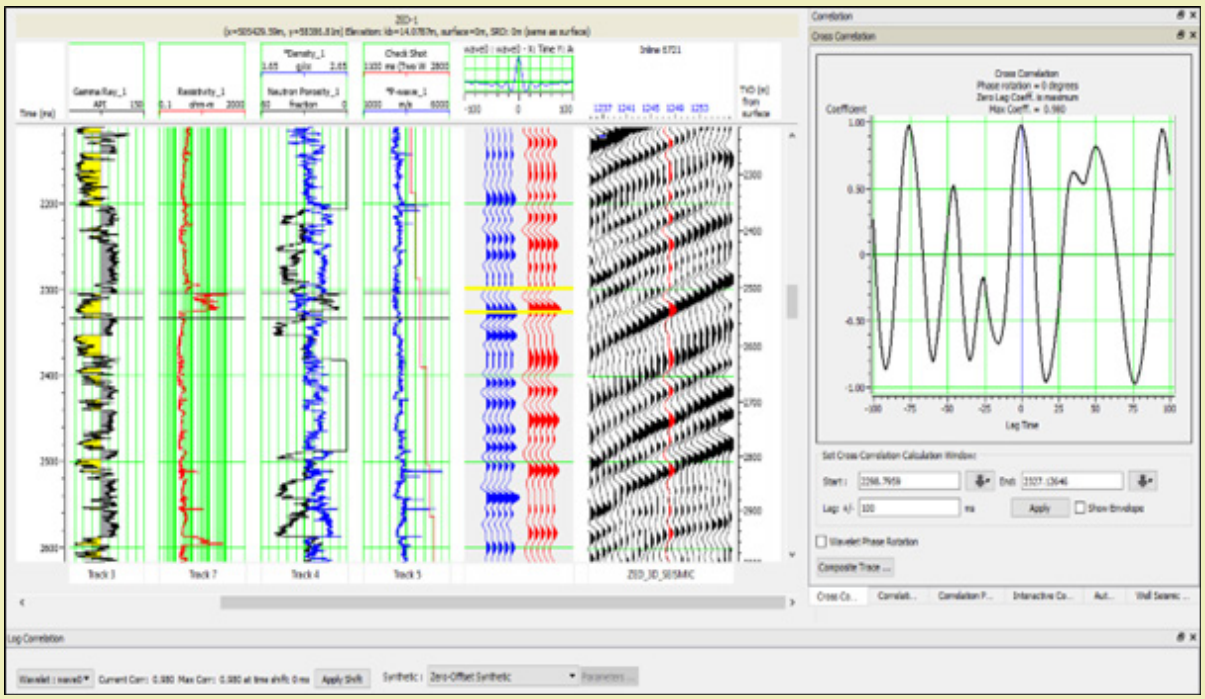

Figure 6: Seismic to well correlation with correlation coefficient of 0.980 (98.0 %) at time shift of 0.00ms down

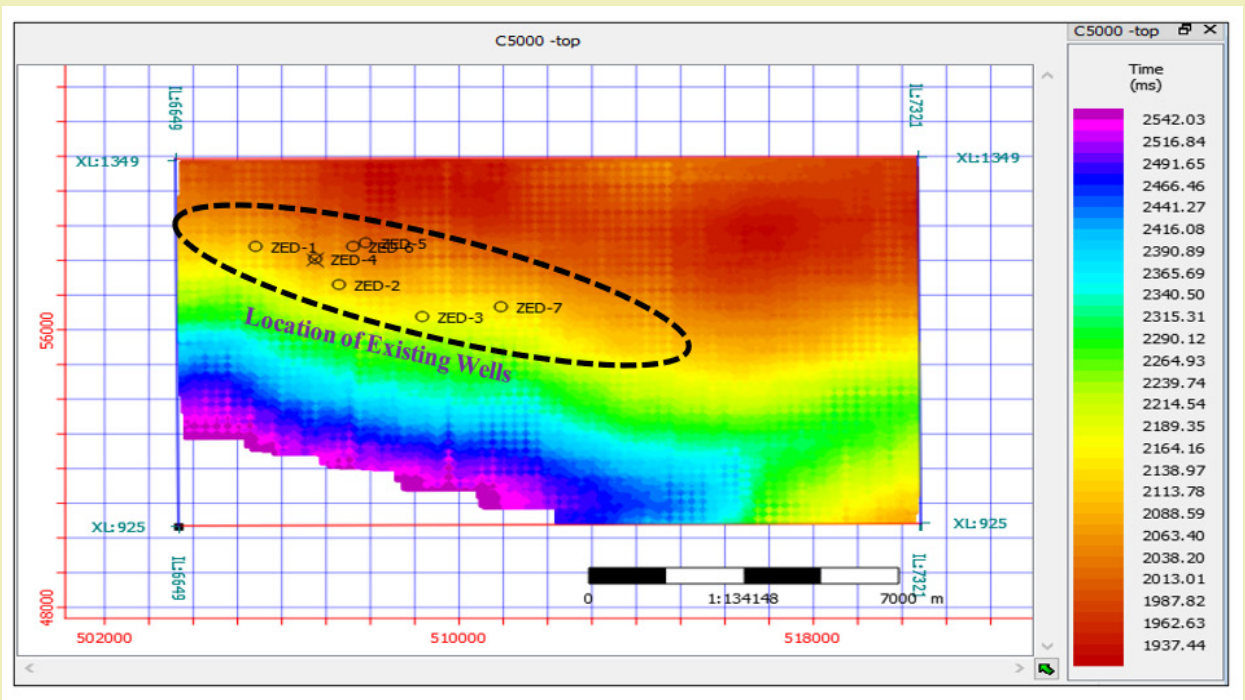

Figure 7: Horizon mapping with Interpolated Picks. Showing reservoir C5000 top and location of the wells

Initial P-Impedance model, Model analysis and inversion

The initial P-impedance model was created based on the density and P-wave velocity values calculated at log resolution from the control well (ZED-1). The initial P-impedance model was used as one of the inputs for the inversion analysis process. The results (p-impedance logs) were then combined into the post-stack volumes and extrapolated throughout the survey domain.[7] Low frequencies are absent from seismic data because they are band-limited. When quantitatively inverting an acoustic impedance dataset and other reservoir parameters that are susceptible to lithofacies variations, low frequency information is essential. This makes it more difficult for the inverted impedance dataset to have the impedance structure needed to accurately represent the behavior of actual underlying rocks, which is essential for producing accurate geological interpretations. In order to make up for this, we included the low frequencies that were absent from the seismic bandwidth and constrained our inversion by using well logs from the ZED-1 well, which contain low to extremely high frequency data. As the first guess model for the conjugate gradient perturbation of the impedance model, this low frequency model was validated using well logs.[7] The inversion outcome is guaranteed to be consistent with the underlying geological trend by the low frequency model. Ultimately, the complete 3D data volume was subjected to a model-based inversion approach. It makes sense for this operation to take note of the wavelet's absolute amplitude. This was resolved by convolving the unscaled wavelet W with the initial model's reflectivity (r) at the well (ZED-1) and correlating it with W^T to produce W^TWr.[19] This produced an inverted density and P-impednce (Zp) volume, which were then interpreted. Crossplots were created between the inverted P-impedance log and the original P-impedance log and between the original P-impedance log and the initial model P-impedance log in order to assess the consistency between the P-impedance logs. The correlation coefficients were then calculated in order to assess their convergence level and log resolution. In order to demonstrate the lateral variation of acoustic impedance at the well locations and away from the well locations, a time slice of inverted P-impedance was derived from the impedance volume at the top and bottom of reservoir C5000 between inlines 6649 and 7321 and crosslines 925 and 1348.

Results and Discussions

The initial density model and initial P-Impedance log at crossline 1248 are shown in Figure 8, together with the gamma-ray log of the control well (ZED-1). The initial P-impedance and density models' color variations exhibit amplitudes that correlate to density ranges of 1.9379 to 2.4021g/cc and P-impedance ranges of 3801 to roughly 11073 ft/s*g/cc, all of which generally rised with depth.

The P-impedance inversion analysis at the well ZED-1 location is displayed in Figure 9. Figure 9 displays the original P-impedance log (blue), the inverted P-impedance log (red), and the first P-impedance model log (black). As shown in Figure 9a, the three logs matched nicely at the top and base of reservoir C5000. At the well location, there was a strong connection between the synthetic (red) and seismic trace (black), yielding an almost perfect correlation of 0.998109 (≈ 99.8%). The calculated error was 369.48, or roughly 6.16 percent, or (0.0616932). The crossplots between the P-impedance logs are shown in Figures 10a and 10b. Figure 10b displays the plot of the original P-impedance log and initial slope coefficients (R^2 of 0.94), whereas Figure 10a displays the plot of the P-impedance log and inverted P-impedance log.

With a gamma ray log from the control well (ZED-01) inserted to show the top and base of reservoir C5000, Figure 11a, 11b, and c displays the initial model density, initial model P-Impedance, and the inverted P-impedance strucrure along inline 6703, crossline 1248 of the 3D seismic data at seismic time 1805.97ms. Both the inverted P-impedance Figure 11c and the original P-impedance model Figure 11b exhibit color variation with amplitudes that match P-impedance (Zp) values ranging from 3801 to 11073m/s*g/cc in both impedance structures. As a result, there is a correlation between the original model P-impedance Figure 11b and the inverted P-impedance Figure 11c.

In particular, compared to the input seismic data Figure 12a, a low-impedance structure at the reservoir window Figure 11 b, 11c as indicated) can be mapped laterally away from the control well. It is possible to forecast lateral changes in lithology and Poisson's ratio by analyzing the P-impedance volume. According to Dubey and Kharagpur,[3] P-impedance, which is the product of rock density and velocity, attenuates as seismic waves come into contact with hydrocarbon-charged sands. For this reason, the inverted attribute may offer litho-fluid information within existing reservoirs as well as help define potential hydrocarbon zones away from the control well.

The input seismic data with a synthetic trace added and the inverted P-impedance section with a P-impedance log computed from the control well (ZED-1) are displayed in Figure 12a, 12b. Low impedance values near the reservoir window are suggestive of the existence of a statigraphic feature, such as a channel that frequently has massive hydrocarbon accumulations. Laterally, the stratigraphic channel can be traced away from the control well in comparison to the input seismic data Figure 12a. The sediment thickness in the channel is said to fluctuate.

Figures 13a and 13b show P-impedance slice outputs at top and base of reservoir C5000 centered at 10ms window. The Impedance slices were extracted from the P-impedance volume at Inline 6703 centered at the well control at top and base of the reservoir. The behavior of the impedance slices correlates well at the top and base of reservoir C5000 Figure 13a, 13b. In both slices low impedance values were observed in the vicinity of the existing wells (as indicated by the black broken circles). In general, hydrocarbon-

charged sands are defined by low density and low impedance values. The impedance slices also showed low impedance values away from the existing wells which are indicative of hydrocarbon prospects (as indicated) that can be exploited for improved hydrocarbon recovery and field development Figures 13a and 13b. These findings show that the seismic inversion process is a suitable procedure for prediction of lateral variations in rock attributes (impedance or density) which are functions of lithology at well control and away from the existing wells. The high impedance zones indicative of shale lithofacies were also defined at the top and base impedance slices as indicated in Figures 13 a and b. The inverted attributes could provide litho-fluid and lithofacies information away from existing reservoirs and this is invaluable in delineating potential hydrocarbon prospects often bypassed during drilling thus, optimizing hydrocarbon recovery and field development. This aids in reservoir management decisions.

In this study, attempt was made to extract porosity values from the inverted P-impedance volume. The extracted porosity values were plotted against P-impedance and colour coded with gamma-ray (GR) log Figure 14. The slope coefficient (regression coefficient $\mathbf{R^2}$ of 0.81) was obtained Figure 14 with an error level of 2.799 which is low and consistent within the acceptable limits of error. From the gamma-ray colour code the sand and shale intervals were defined (as indicated).

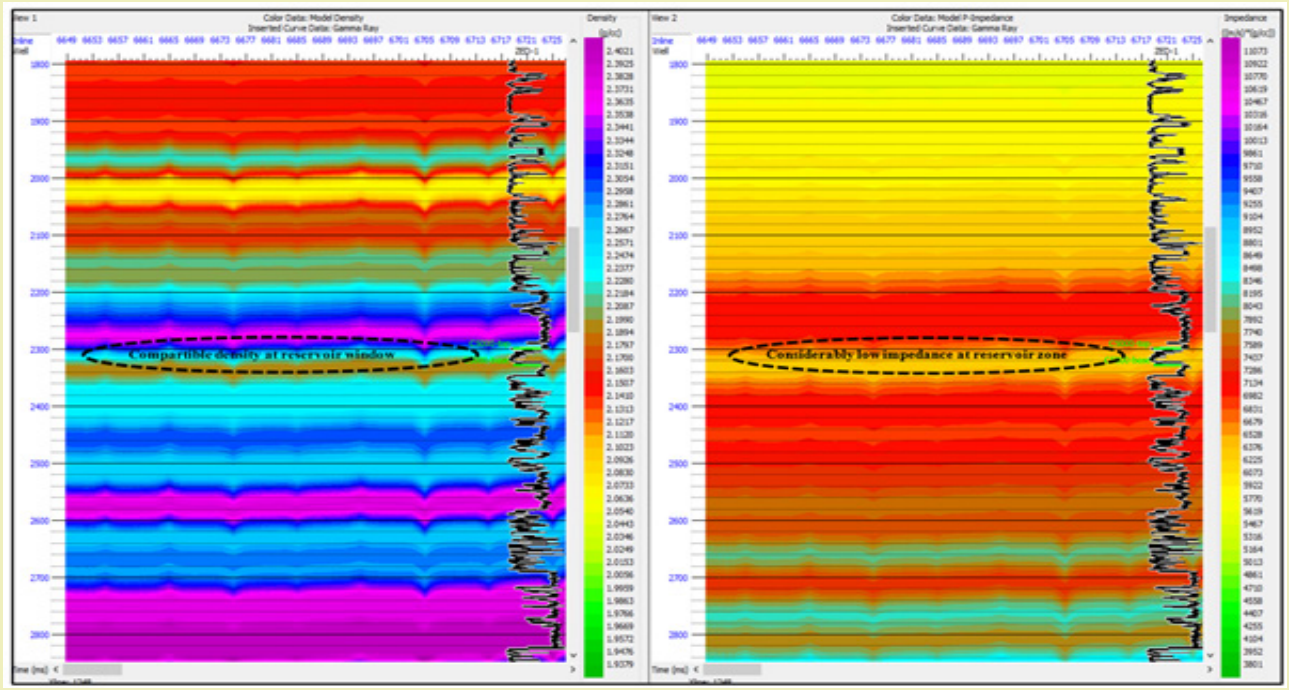

Figure 8: Initial model of density log and P-Impedance log at Xline 1248 with insertion of gamma-ray log in the vicinity of the control well (ZED-01)

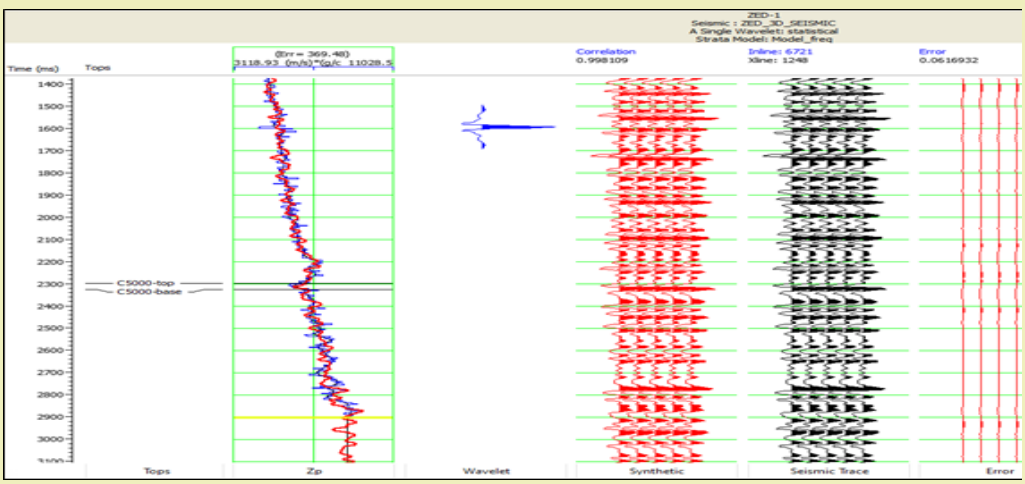

Figure 9: Analysis of P-impedance inversion at well ZED-01: Initial P-impedance model log (black), original P-impedance log (blue), and inverted P-impedance log (red)

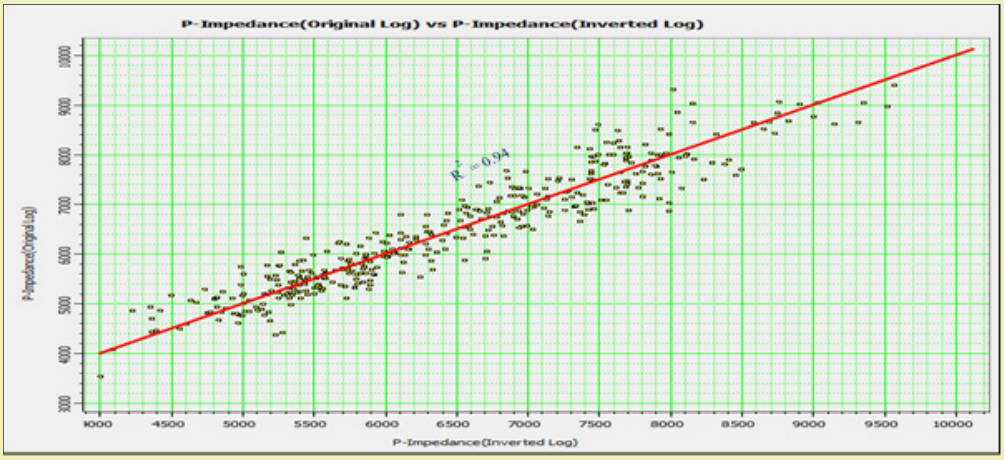

Figure 10a: Plot of original P-impedance log versus Inverted P-impedance log

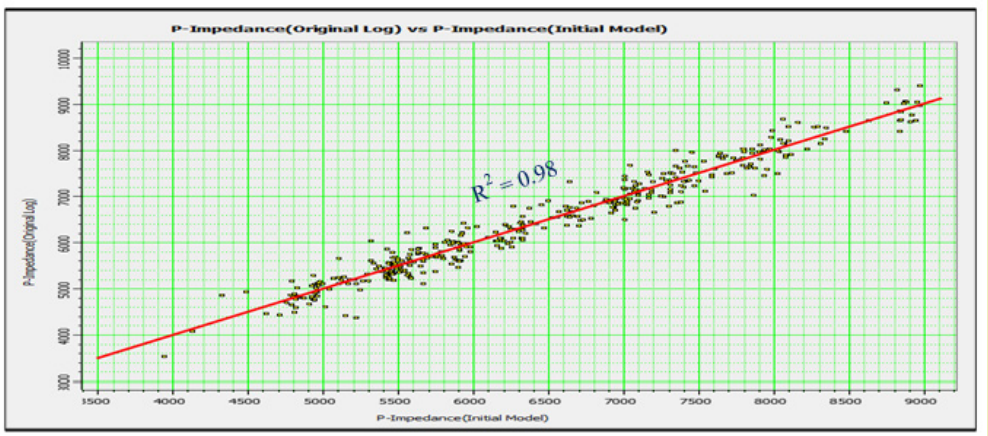

Figure 10b: Plot of original P-impedance log versus Initial model P-impedance log

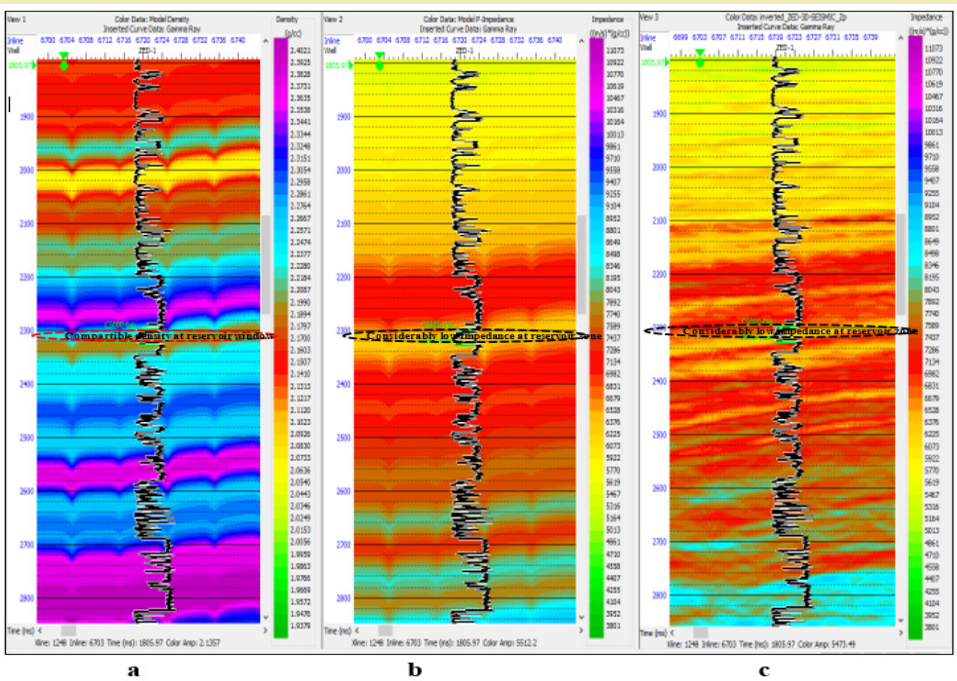

Figure 11: Inversion Analysis with a correlation of 0.998 and error of 0.06 a: Initial model of density; b: Initial model of P-Impedance volume; c: Inverted P-impedance volume in the vicinity of the control well (ZED-01) as indicate

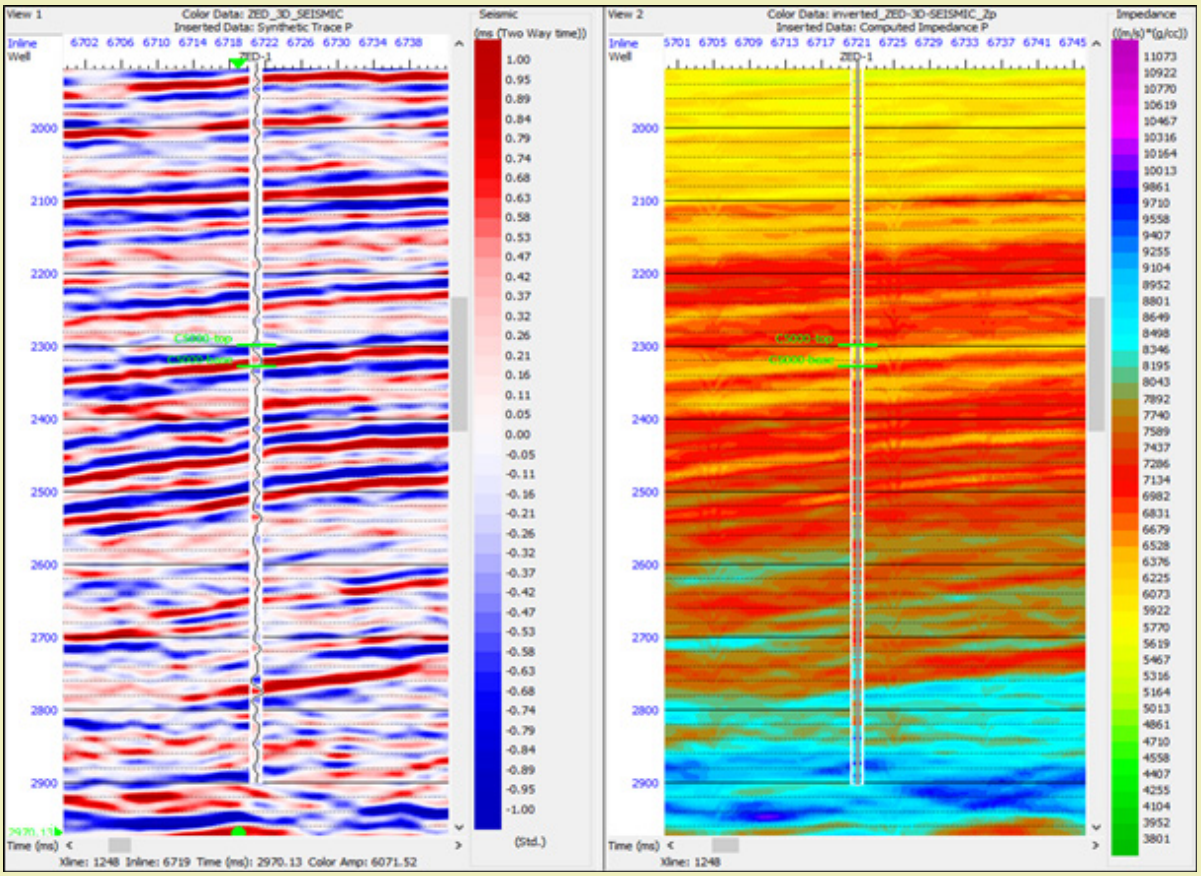

Figure 12: Inversion Analysis with a correlation of 0.998 and error of 0.06. **(a)** seismic input at inline 6719 **(b)** inverted P-impedance of input seismic

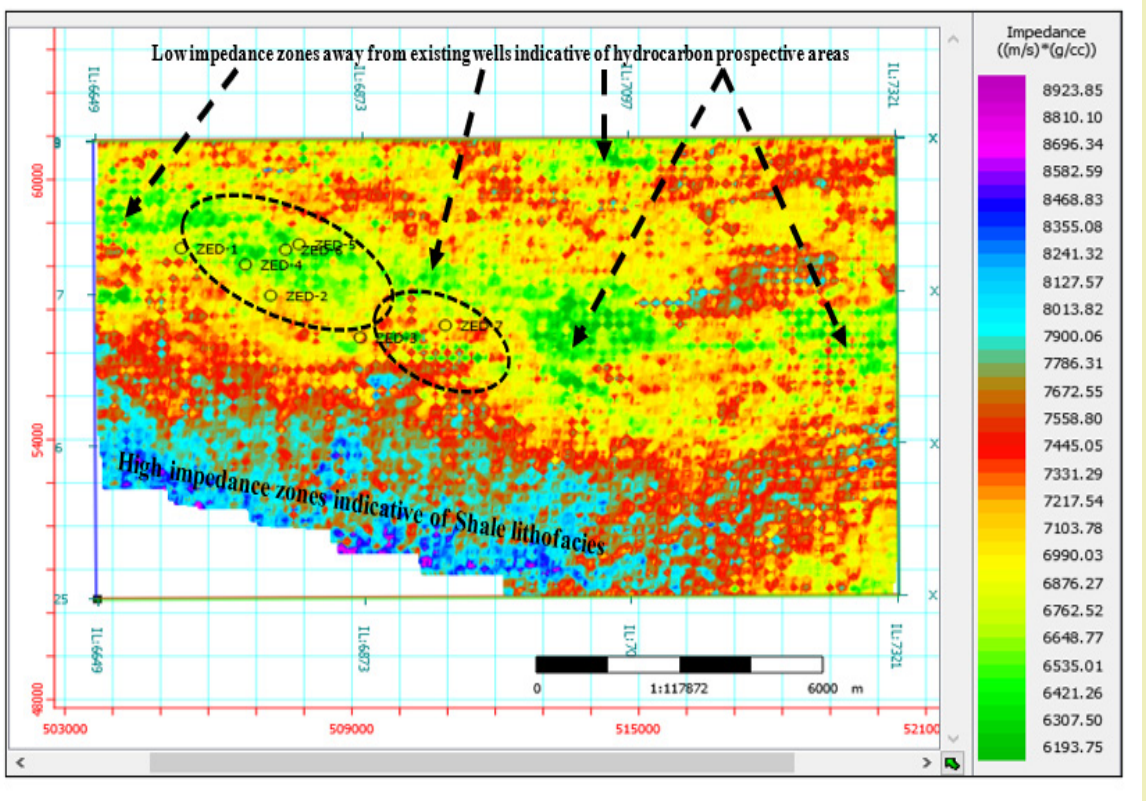

Figure 13a: Inversion Analysis: P-Impedance Time Slice at top of reservoir C5000

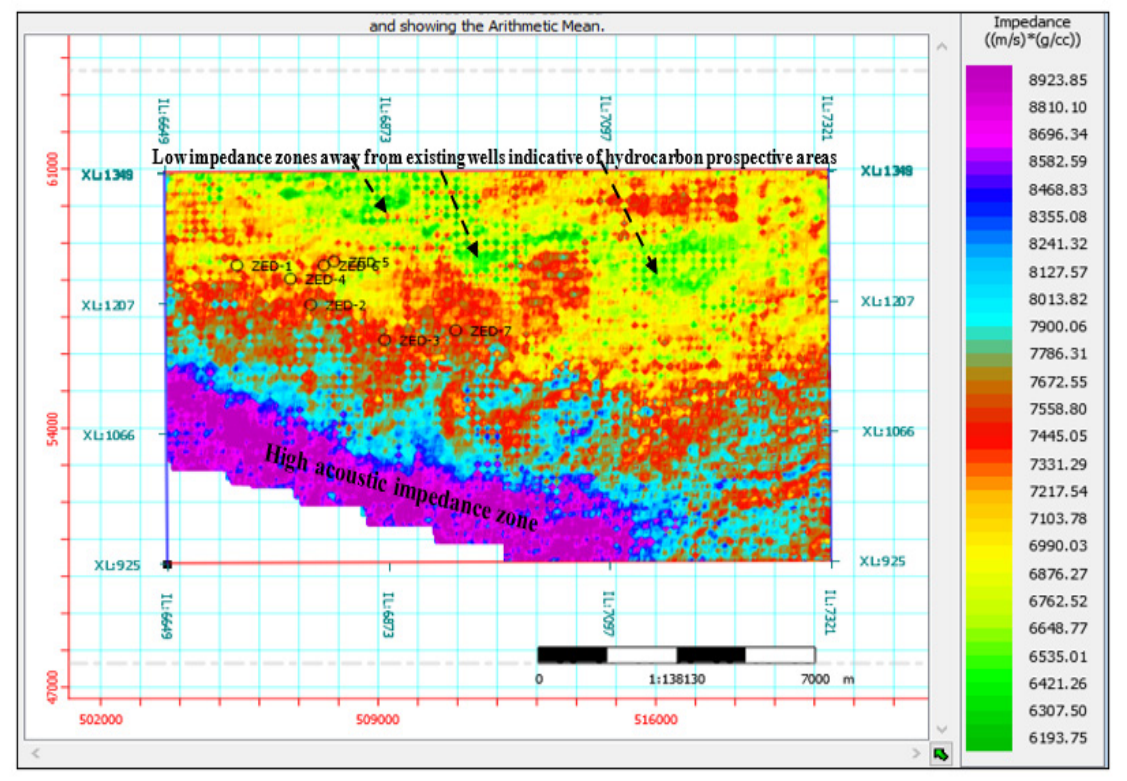

Figure 13 b: Inversion Analysis: P-Impedance Time Slice at base of reservoir C5000

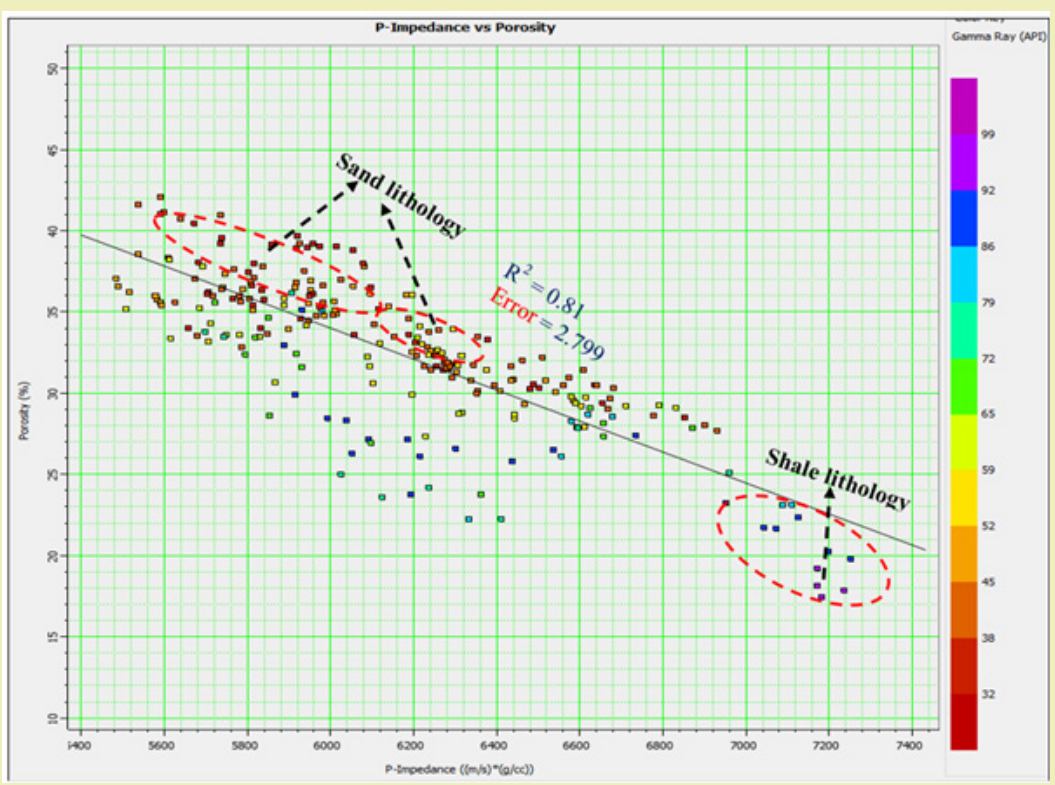

Figure 14: Inversion Analysis: Crossplot of Porosity (%) against inverted P-Impedance of Reservoir C5000 colour coded with Gamma Ray (GR-Log) for lithology delineation

Conclusion

In order to optimize hydrocarbon recovery, a model-based method of post-stack seismic inversion was applied to 3D seismic data from ZED-Field offshore Niger Delta. The goal was the lateral prediction of rock properties.

The following conclusions are achieved:

1. To produce the P-impedance structure, the inversion analysis procedure reverses the convolution of the source wavelet and the reflectivity of the earth. An impedance structure with a near-perfect correlation of 99.8% at 0.0616 error (6.16%) was realized by P-impedance analysis, demonstrating an excellent fit between the initial-model impedance log, the inverted impedance log, and the original impedance log.
2. The inversion analysis between the initial-model density, initial-model impedance and inverted impedance showed low density and impedance values at the vicinity of reservoir C5000. This observation is theoretically compatible for hydrocarbon-charged sand.
3. P-impedance slices extracted at the top and base of reservoir C5000 clearly showed low impedance values away from the existing wells which are indicative of new hydrocarbon prospects that can be explored for improved hydrocarbon recovery and field development.
4. The findings demonstrate that acoustic impedance inversion is a true technique for defining lateral changes in lithology-related rock parameters (acoustic impedance and density). The technique identified dispersed areas of low acoustic impedance, which may be connected to the seismic input data to enhance the interpretability of reservoir properties. These zones may also be integrated with seismic stratigraphy to enable more accurate reservoir prediction beyond the control wells.

Acknowledgments

We wish to express our gratitude to Shell Petroleum Development Company (SPDC) Nigeria for providing the dataset used for this study and to CGG Geosoftware for providing the software used for the study.

Funding

This Research Article received no external funding.

Conflicts of Interest

Regarding the publication of this article, the authors declare that they have no conflict of interest.

References

1. Karbalaali H, Shadizadeh SR, Ali R. Delineating hydrocarbon bearing zones using Elastic Impedance Inversion a persian Gulf example. *Iranian J Oil and Gas Science and Technology*. 2013;2(2):8-19.
2. Hansen TM, Mosegaard K, Pedersen Tatalovic R, et al. Attribute-guided well-log interpolation applied to low-frequency impedance estimation. *Geophysics.* 2008;73(6).
3. Dubey AK. Reservoir characterization using AVO and seismic inversion techniques. *9th Biennial International Conference & Exhibition on Petroleum Geophysics, Hyderabad*. 2012.
4. Parvaneh K. Structure-constrained relative acoustic Impedance using Stratigraphic Co-ordinates. *Geophysics.* 2015;80(3):63-67.
5. Eze S, Orji OM, Nnorom SL, et al. Model Based Inversion of Acoustic impedance from Seismic trace for Lithofacies Differentiation: An Application in XY Field Offshore Niger Delta. *J of Appl Sci Environ Manage (JASEM).* 2019;23(9):1677-1684.
6. Ogagarue DO, Alaminiokuma GI. Lateral Rock Property Prediction by Post Stack Acoustic Impedance Inversion: A case study from offshore Niger Delta. *Int J of Sci Basic and Appl Research (IJSBAR).*2016;26(3):1-13.
7. Jason M, Crank MC, Don L. Acoustic impedance inversion and Co_2 flood detection at the Alder flats ECBM Project. *CREWES Research Report*. 2008;20.
8. Lavergne M, William C. Inversion of seismograms and pseudo-velocity logs. *Geophys Prosp.* 1977;25:232-250
9. Lindseth RO. Synthetic sonic logs-a process for stratigraphic interpretation. *Geophysics.* 1979;44(1): 3-26.
10. Short KC, Stauble AJ. Outline of geology of Niger Delta. *AAPG Bulletin*. 1967;51(5):761-779.
11. Asseez OL. Review of the stratigraphy, sedimentation and structure of the Niger Delta. In: Kogbe (ed) Geology of Nigeria. Rock View (Nig.) Ltd., Jos. 1989:pp.311-324.
12. Ideozu RU, Iheaturu TC, Ugwueze CU, et al. Reservoir properties and sealing potentials of the Akani Oil Field structures, Eastern Niger Delta, Nigeria. *Journal of Oil, Gas Petrochem Sciences*. 2018;1(2):56–65.
13. Doust H, Omatsola E. Niger Delta. In: Edwards, J.D. and Santogrossi, P.A., Eds., Divergent/Passive Margin Basins. *AAPG Memoir 48, American Association of Petroleum Geologists,* Tulsa. 1990:pp.239-248.
14. Merki PJ. Structural geology of the Cenozoic Niger Delta. University of Ibadan Press, Ibadan. 1970:pp.251-268.
15. Giadom FD, Akpokodje EG, Tse AC. Determination of migration rates of contaminants in a hydrocarbon-polluted site using non-reactive tracer test in the Niger Delta Nigeria. *Environmental Earth Sciences.* 2015;74:879-888.
16. Cooke D, Schneider W. Generalized inversion of reflection seismic data. *Geophy*sics. 1983;48(6):665-676.
17. Auster RC, Borchers B, Thurber CH. Parameter estimation and inverse problems. *Elsevier Academic Press*. 2005.
18. Ahmed H, John C. Distinguishing gas-bearing sandstones reservoirs within mixed Siliciclastic-Carbonate sequence using extended elastic impedance: Nile Delta, Egypt. *Interp.* 2016;4(4):435-449.
19. Hampson D, Russell B. First break interpretation using generalized linear inversion. *Journal of the Canadian Society of Exploration Geophysicists.* 1984;20(1):40-54.